Robotics & Automation Engineering Journal
ISSN: 2577-2899

Juniper Publishers
key to the Researchers

Research Article
Volume 4 Issue 4 - June 2019
DOI: 10.19080/RAEJ.2019.04.555641

Robot Autom Eng J
Copyright © All rights are reserved by Gareth J Monkman

Smart Stiction

Gareth J Monkman*, Dirk Sindersberger, Nina Prem and Tamara Szecsey

Mechatronics Research Unit, OTH-Regensburg, Germany

Submission: May 27, 2019; **Published:** June 27, 2019

***Corresponding author:** Gareth J Monkman, Mechatronics Research Unit, OTH-Regensburg, Germany

Abstract

Soft robotics could loosely be described as the engineering science of expanded dexterity through controllable flexibility. The exploitation of controllable compliance through the judicious choice of soft flexible members, as opposed to a finite number of rigid kinematic joints, can result in greater dexterity without compromising simplicity. One example is the replacement of segmented mechanical legs with simple compliant material eruciform prolegs. To achieve this in robotics, without introducing additional mechanical joints, mobile surfaces with switchable coefficients of friction is essential. This paper explains how, using silicone based smart materials, the rapid alternation between kinematic and static friction (stiction) may be achieved.

Introduction

Stiction (sometimes referred to as "stick-slip") is a word construction derived from friction and sticking. It represents the forces due to static friction which manifests itself as a cohesion force threshold which must be overcome to enable relative motion between otherwise stationary objects in contact [1]. Following the onset of movement, resistance to motion is provided exclusively by dynamic friction. In engineering, stiction is usually considered to be a problem [2]. However, in certain applications, stiction can be deliberately implemented to advantage, as in the case of soft robotics where movement is to be achieved through controlled sliding rather than rolling or crawling. It is not easy to make a clear distinction between adhesion and stiction. Both are related to inter molecular viscoelastic effects and both are influenced by surface roughness. Adhesion (for example magneto adhesion and electro adhesion) concerns the application of an astrictive force which causes prehension whereas magnetostriction and electrostriction pertain to the control of friction though a magnetic or electric field respectively. Should it not be possible to sustain post contact retention on lifting, then adhesion properties are absent. If, despite this, the frictional coefficient is still controllable by means of some external influence, then stiction is present.

The coefficient of static friction μ_s denotes the necessary frictional force between two surfaces in order to maintain two objects relative to one another immobile (1).

$$|F_s| \leq \mu_s |F_N| \quad (1)$$

Once the applied force exceeds the maximum static frictional force, sliding will commence. The force due to kinetic friction (2) always opposes the direction of motion.

$$|F_k| = \mu_k |F_N| \quad (2)$$

In expressions (1) and (2) FN is the force (usually due to gravity, F_N = m g) normal to the direction of motion. The surfaces of highly polished planar objects tend to adhere to one another. This is often attributed to electrostatic and/or Van der Waals forces. After overcoming the initial stiction forces, relative motion occurs, and the resistance shifts into the kinetic region as shown in Figure 1. Should the movement direction be reversed, then a degree of positional hysteresis will be experienced.

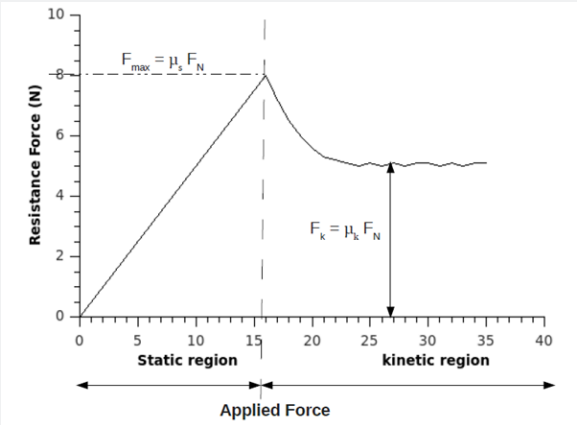

Figure 1: Typical static and kinetic friction regions.

F_N is a function of gravity and is otherwise only dependent on mass. However, F_N can be increased by the application of additional force, though this is not necessarily advantageous. What is important is the relationship between μ_s and μ_k.

$$\frac{\mu_s}{\mu_k} \geq 1 \quad (3)$$

In order to increase the relationship in (3), the mechanical characteristics of one or both contacting material surfaces must be precisely controlled. There are several relevant factors here.

Frictional Materials

Before introducing magnetically and electrically controllable friction, it pays to consider the frictional coefficients of general engineering materials. These are commonly available in almost any mechanical engineering textbook [3]. The values given are usually in the range 0 (no friction) to 1 (the frictional force is equal to the normal force F_N). Mechanically compliant materials such as rubbers demonstrate some of the highest frictional coefficients. In fact, silicone rubbers can have frictional coefficients higher than unity [4]. What is required is a manner in which these coefficients can be changed by means of an external influence.

Compliance is the inverse of stiffness or the potential of a surface to elastically change its geometry to comply with a different topology. The ability to switch between two elastic states is the basis of shape memory materials [5]. In the form of a practical device, what is ideally needed is a switchable mating surface, where in one condition the surface has a high elastic modulus and a very low coefficient of friction (similar to PTFE) and in the other condition is extremely compliant and has a high coefficient of friction (like silicone rubber).

In a real situation, the entire area of a compliant surface is not in contact with the rigid surface over which it is intended to propagate. The compliant mating surface contains a plurality of approximately semi-spherical asperities, which may or may not be in contact with the lower surface. This is illustrated in Figure 2.

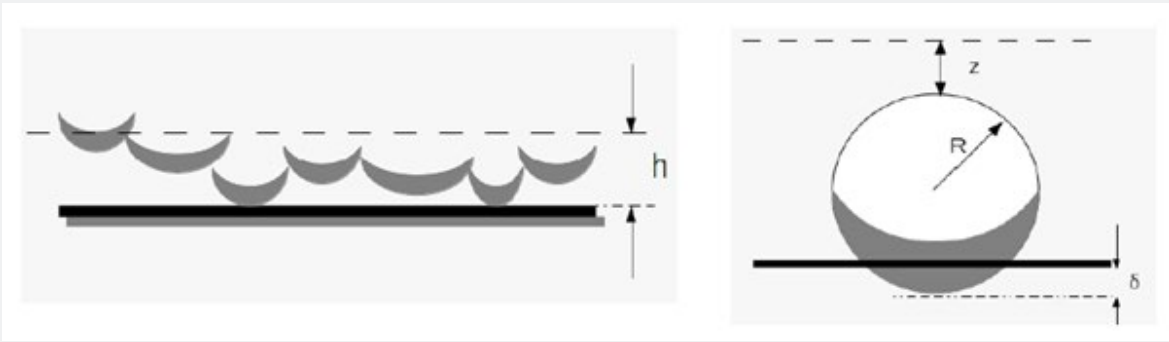

Figure 2: a) Asperities over a surface b) a single asperity in contact with a surface.

Given a nominal height between the two surfaces h, as shown in Figure 2a, then only a small amount of asperity will be in direct contact with the lower planar surface. Figure 2b illustrates the situation for a single asperity with curvature radius R and displacement z from the reference plane. At the point of contact, the elastic asperity will deform with displacement [6].

Given a random variation in height h following a Gaussian probability distribution, then the probability of contact is given by (4).

$$P(z > h) = \int_h^\infty \Phi(z)dz \quad (4)$$

The number of contacts n can be calculated from the amount of asperity N (5).

$$n = N\int_h^\infty \Phi(z)dz \quad (5)$$

Using Hertz's theory, the area of contact between the surface and an asperity with displacement z is given by expression [7] (6).

$$\pi P\delta = \pi R(z-h) \quad (6)$$

The area of contact (7) and the contact force {8} may be calculated accordingly [6].

$$A = \pi RN\int_h^\infty (z-h)\Phi(z)dz \quad (7)$$

For the two mating surface materials, E_1 and E_2 are the elastic moduli and ν_1 and ν_2 are the respective Poisson's ratios.

$$F = \frac{4}{3}\pi N\sqrt{R}\left(\frac{E_1}{1-\nu_1^2}+\frac{E_2}{1-\nu_2^2}\right)\int_h^\infty (z-h)^{3/2}\Phi(z)dz \quad (8)$$

For an individual contact point, dividing (8) by (7), gives the load pressure (9).

$$\sigma = \frac{4}{3\sqrt{R}}\left(\frac{E_1}{1-\nu_1^2}+\frac{E_2}{1-\nu_2^2}\right) \quad (9)$$

The greater the effective elastic modulus, the higher the applicable load pressure. A lower elastic modulus results in a correspondingly lower pressure for a given deformation-compliance. When one of the surfaces is highly compliant, then R also becomes a function of the applied pressure. Transposing for R in (9) and differentiating gives (10).

$$\frac{\partial R}{\partial \sigma} = \frac{-16}{18\sigma^{3/2}}\left(\frac{E_1}{1-\nu_1^2}+\frac{E_2}{1-\nu_2^2}\right) \quad (10)$$

The function (10) tends to zero for large values of pressure, thus making the effect stable. Furthermore, for a given surface, either E_1 or E_2 will be rigid and constant. The other must be controllable in accordance with (3). Halling [3] also provides a

How to cite this article: Gareth J Monkman, Dirk Sindersberger, Nina Prem, Tamara Szecsey. Smart Stiction. Robot Autom Eng J. 2019; 4(4): 555641. DOI: 10.19080/RAEJ.2019.04.555641

similar analysis for conical asperities but for the sake of brevity this will not be included here [3].

Clearly, given a composite material with two sets of controllable asperity, one with a high and one with a low frictional coefficient, the criteria for a practical device laid out earlier, is achievable. This principle already exists in nature. Eruciform lifeforms employ soft prolegs with hard crochets on the ends to allow switching between sliding and prehension. Although the Gecko foot enjoys the ultimate natural prehension, it does not adhere to a PTFE surface [8]. Furthermore, the objective in soft robotics is to achieve this without resorting to direct methods of mechanical alternation.

Magnetostiction

Here it must be distinguished between magneto adhesion and magnetostiction. The former concerns simple magnetic force produced when a magnetic field is applied against a ferrous surface, while the latter relates to frictional changes in the properties of a material caused by the application of a magnetic field. When the coefficient of static friction s is a function of an applied magnetic field, then the resulting force which resists motion is the product of this frictional coefficient m and the normal force F_N. Magnetostiction should also not be confused with magnetostriction. The latter refers to a second order magneto-mechanical effect which leads to reversible dimensional changes in specific magnetic materials [9].

Magnetoactive polymers (MAP) are polymer matrices containing a dispersion of ferromagnetic or paramagnetic particles distributed within a soft, nonmagnetic elastomer [10]. Their mechanical [11] and electrical [12,13] properties have been extensively investigated. Under the influence of a magnetic field gradient, both magnetodeformation and an increase in elastic modulus results [14]. Magnetodeformation can result in extremely large displacements as is exploited in the design of origami actuators [15].

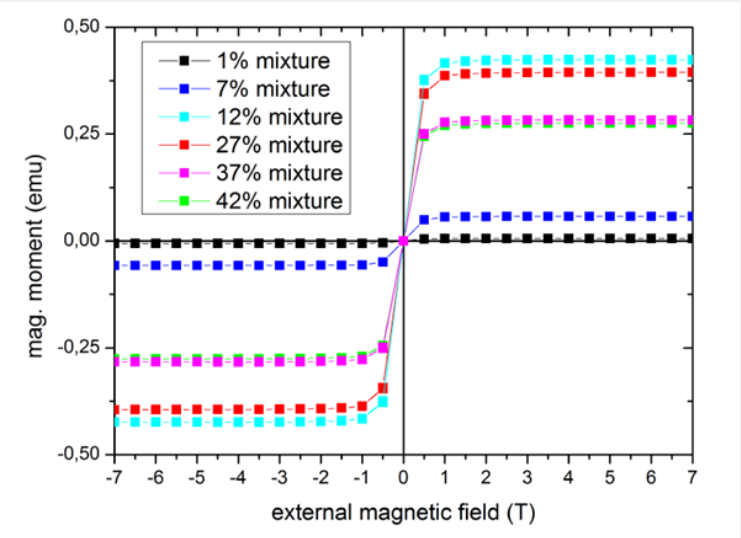

Figure 3: Magnetic moment for MAP with different CIP content.

If E_1 or E_2 in (9) is a function of the applied magnetic field, as in the case of a magnetoactive polymer [14], then the criterion outlined in (3) can be, at least partly, fulfilled. However, the bulk permeability of a magnetoactive polymer changes with mechanical deformation. This, in turn, changes the magnetic flux density in the medium and with it the degree of deformation [16]. Magnetizations measurements carried out on $1mm^3$ samples from the same production batch using a SQUID magnetometer (Quantum Design MPMS XL) including MPMS RSO Controller and digital R/G Bridge can be seen from Figure 3. Although the maximum carbonyl iron powder (CIP) concentration does not coincide with the maximum magnetization (which occurs between 12%wt and 27%wt CIP), a compression of the MAP will inevitably result in a localized increase in CIP.

The inclusion of hard magnetic particles allows the MAP to be permanently magnetized [17]. For example, Nd-Pr-Fe-Co-Zr-Ti-Bm, SmCo or NdFeB are materials commonly used in modern permanent magnets. Because of potential oxidation, the finished magnets are usually chrome or epoxy resin coated. As well as providing the elastic matrix, the polymer in a MAP serves the same purpose. Unfortunately, this introduces a slight problem. Profiling of a MAP surface alone rarely suffices as it is impossible to use the magnetic particles themselves as asperities [18]. Inevitably in a MAP each magnetic particle is surrounded by a thin layer of polymer, so the friction coefficient remains the same with or without magnetic field. Magnetic particles not completely surrounded by the polymer matrix rapidly detach themselves from the matrix thus playing no further role in the dynamics of the system. In addition, although immediately after magnetization, each of the particles are magnetized in the same direction, this situation rapidity changes as the magnetized particles attempt to rotate within the polymer matrix in order

How to cite this article: Gareth J Monkman, Dirk Sindersberger, Nina Prem, Tamara Szecsey. Smart Stiction. Robot Autom Eng J. 2019; 4(4): 555641. DOI: 10.19080/RAEJ.2019.04.555641

to reach the level of lowest energy [19]. This effect can be clearly seen using a magnetic field camera (Matesy MagView) in Figure 4a which shows the magnetic flux density over the surface of a hard-magnetic MAP immediately following magnetisation and Figure 4b the same MAP several hours later where a substantial portion of the particle orientation has changed.

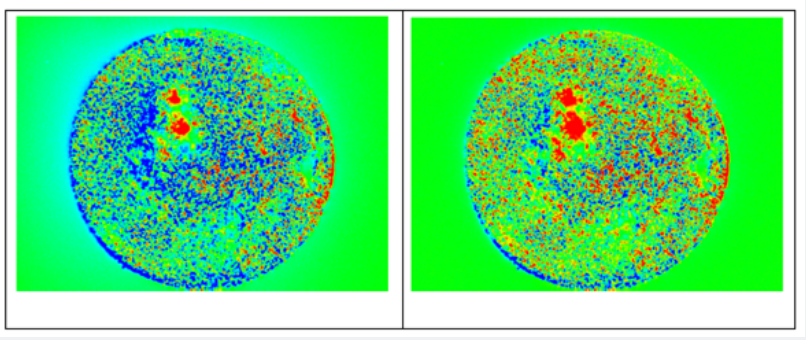

Figure 4: Magnetic flux distribution a) immediately after magnetization; b) after several hours.

In order to create an effective switchable stiction device with two frictional states, two discrete areas of the same substrate having different frictional coefficients must be presented. A number of potential physical implementations exist, the most effective of which are bistable devices [15] similar to the previously mentioned insect prolegs. One portion of the device comprises highly compliant addition-curing RTV-2 silicone (Wacker Silicones) polydimethylsiloxane (PDMS) elastomer sans magnetic content which exhibits a high coefficient of friction between its under-surface and any surface in which it comes into contact with. The other portion is magnetically active and hardens under the influence of the magnetic field thus providing a lower frictional coefficient and less compliance. This may also be augmented by a metallic or PTFE layer to further reduce friction.

The traditional means of ascertaining frictional coefficients is the tilted plane method, where an object is placed on a sloped surface and the slope angle gradually increased. Static friction resistance develops when the object starts sliding [20]. At a given time, the ratio between the load applied at right angles to the sloped surface (W) and the friction resistance (F) is called the coefficient of friction (f) and is determined according to the following equation:

$$f = F/W = TAN(\theta) \quad (11)$$

Much more accurate results may be obtained by measuring the force threshold at the point of movement. Replacing F_N with mg in (1) and transposing for s gives (12).

$$\mu_s = \frac{F_s}{mg} \quad (12)$$

Preliminary experiments were conducted on such a device comprising two interspaced surface structures effectively selectable by means of a magnetic field.

Experimental

A 6 axis Staübli RX60 [21] industrial robot equipped with an ATI FTN-Mini40 6 d.o.f. force/torque sensor provided linear movement of such a bistable element in both active and inactive states [22]. Figure 5 shows the measured force in the Y-axis (direction of movement) and the Z-axis (normal to the direction of movement) for a linear displacement in the Y-direction. Because compressive stress is by convention negative, the values of force in the Z-axis of Figure 5 have been inverted.

The slight decrease in F_y at the beginning of movement is the initial changeover from static to dynamic friction of the sliding condition. The deliberate change from low to high friction occurred at increment 4 along the abscissa of Figure 5.

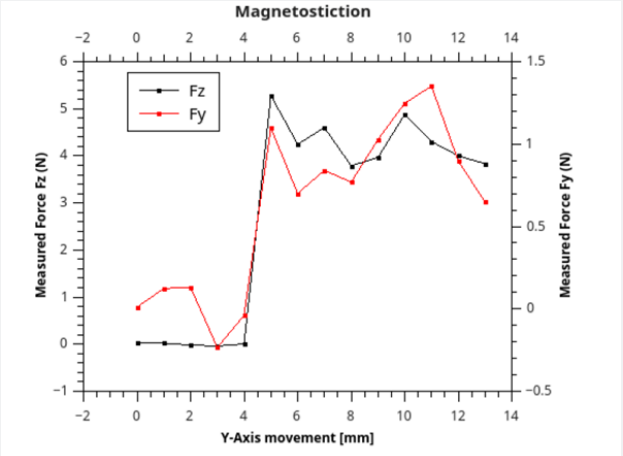

Figure 5: Force measured in the Y and Z axes during motion.

Conclusion

Controllable stiction, as described in this paper, can be implemented in many possible ways. The manipulation of mechanical asperities on a surface can give rise to controllable friction. However, this can only be achieved by the application of some external influence such as an applied magnetic or electric field. This paper has demonstrated how magnetostiction can be implemented through magnetic field induced changes in the mechanical properties, and in particular the elastic modulus, of magnetoactive polymer substrates in order to control the fric-

How to cite this article: Gareth J Monkman, Dirk Sindersberger, Nina Prem, Tamara Szecsey. Smart Stiction. Robot Autom Eng J. 2019; 4(4): 555641.
DOI: 10.19080/RAEJ.2019.04.555641

tion between two surfaces. The application of magnetostiction and its relevance to controllable motion in soft robotics has been demonstrated as a practical example.

Acknowledgement

The authors would like to express their thanks to the German Ministry of Education and Research (BMBF) for financial support for the HASASEM (01IRA14D) and MagElan Projects (13N10573) and the German Research Federation (DFG) for financial support within the SPP1681 (MO 2196/2-1) research program.

References

1. Yamamoto T, Kasamatsu Y, Hyodo H (2001) Advanced Stiction-Free Slider and DLC Overcoat. FUJITSU Sci Tech J 37: 1-11.
2. Ruel M (2000) Stiction: The Hidden Menace: How to Recognize This Most Difficult Cause of Loop Cycling.
3. Halling J (1975) Principles of Tribology. Macmillan Press Ltd, London, UK.
4. Bartlett BW (1994) Coefficients of Friction Greater than Unity. American Journal of Physics.
5. Monkman GJ (2000) Advances in Shape Memory Polymer Actuation. Mechatronics 10(4/5): 489-498.
6. Greenwood JA, Williamson PBJ (1966) Contact of nominally flat surfaces. Proceedings of the Royal Society of London. Mathematical and Physical Sciences 300: 319.
7. Hills DA, Nowell D, Sackfield A (1993) Mechanics of Elastic Contacts. Butterworth-Heinemann, p. 506.
8. Autumn K, Peattie AM (2002) Mechanisms of Adhesion in Geckos. Integr Comp Biol 42: 1081-1090.
9. Lim SH, Kim SR, Kang SY, Park JK, Nam JT, et al. (1999) Magnetostrictive properties of polymer-bonded Terfenol-D composites. Journal of Magnetism and Magnetic Materials 191(1-2): 113-121.
10. Dorfmann A, Ogden RW (2003) Magnetoelastic modelling of elastomers. Eur J Mech A, 22(4): 497-507.
11. Li WH, Zhou Y, Tian TF (2010) Viscoelastic properties of MR elastomers under harmonic loading-Rheol Acta 49(7): 733-740.
12. Bica I (2012) The influence of the magnetic field on the elastic properties of anisotropic magnetorheological elastomers. Journal of Industrial and Engineering Chemistry 18: 1666-1669.
13. Petcharoen K, Sirivat A (2016) Magneto-electro-responsive material based on magnetite/polyurethane composites. Materials Science and Engineering C 61: 312-323.
14. Stoll A, Mayer M, Monkman G, Shamon in M (2014) Evaluation of highly compliant magneto-active elastomers with colossal magnetorheological response. J Appl Polym Sci 131.
15. Crivaro AR, Sheridan M, Frecker TW, Simpson, Von Lockette P (2015) Bistable compliant mechanism using magneto active elastomer actuation. Journal of Intelligent Material Systems and Structures 27(15): 2049-2061.
16. Han Y, Mohla A, Huang X, Hong W, Faidley LE (2015) Magnetostriction and Field Stiffening of Magneto. Active Elastomers. International Journal of Applied Mechanics 7(1): 1-16.
17. Böse. H, Monkman GJ, Freimuth H, Klein D, Ermert H, et al. (2002) ER Fluid Based Haptic System for Virtual Reality. 8th Interntional conf. On ne Actuators, Bremen: Pp. 351-354.
18. Forster E, Mayer M, Rabindranath R, Bentz A, Böse H, et al. (2011) Monkman Surface Control and Characterization of ultra-soft Magneto-Active Polymers (MAP), EuroEAP. First international conference on Electromechanically Active Polymer (EAP) transducers & artificial muscles-Pisa.
19. Sorokin V, Stepanov G, Shamonin M, Monkman GJ, Khokhlov AR, Kramarenko EY (2015) Hysteresis of the viscoelastic properties and the normal force in magnetically and mechanically softmagnetoactive elastomers: Effects of filler composition, strain amplitude and magnetic field. Polymer 76: 191-202.
20. Koch SW, Christman JR, Derringh E (2011) Halliday Physik.
21. Stäubli (1999) RX60 Robot, CS7M controller.
22. Schunk K (2016) F/T Transducer Six-Axis Force/Torque Sensor System Installation and Operation Manual Document #: 9620-05.

This work is licensed under Creative Commons Attribution 4.0 License
DOI: 10.19080/RAEJ.2019.04.555641

Your next submission with Juniper Publishers will reach you the below assets

- Quality Editorial service
- Swift Peer Review
- Reprints availability
- E-prints Service
- Manuscript Podcast for convenient understanding
- Global attainment for your research
- Manuscript accessibility in different formats

(Pdf, E-pub, Full Text, Audio)

- Unceasing customer service

Track the below URL for one-step submission
https://juniperpublishers.com/online-submission.php

How to cite this article: Gareth J Monkman, Dirk Sindersberger, Nina Prem, Tamara Szecsey. Smart Stiction. Robot Autom Eng J. 2019; 4(4): 555641. DOI: 10.19080/RAEJ.2019.04.555641